

## Article

# Synthesis and Characterization of a Self-Crosslinked Organic Copolymer Kappa-Carrageenan/Polyacrylamide/Cetrimide ( $\kappa$ -CAR/PAAm/CI) Hydrogel with Antimicrobial and Anti-Inflammatory Activities for Wound Healing

Fatimah A. Agili \* and Sahera F. Mohamed

Department of Chemistry, Faculty of Science, Jazan University, Jazan 82621, Saudi Arabia; saheramohamed@yahoo.co.uk

\* Correspondence: dr.fatmah2000@gmail.com

**Abstract:** The current study aimed to produce a material that has dual effects of healing and anti-inflammatory activity. For this purpose, a  $\kappa$ -carrageenan/polyacrylamide film loaded with cetrimide ( $\kappa$ -CAR/PAAm/CI) was developed using the manual casting technique. Definite concentrations of  $\kappa$ -CAR and AAm were heated at 80 °C for 2 h, and CI and glycerol were added. The solution was cast without using an initiator or crosslinker. The reaction of the sulfonic acid group  $-\text{SO}_3\text{H}$  of  $\kappa$ -CAR with the  $-\text{CONH}_2$  group of PAAm lead to the formation of a sulfonamide ( $-\text{SO}_2\text{NH}-$ ) group. The characteristics of the produced films were investigated based on FT-IR, TGA, the contact angle, and mechanical properties. An improvement in the thermal stability of the  $\kappa$ -CAR/PAAm/CI<sub>2</sub> film containing 1.5% CI was achieved, compared to the film with 0.5% CI ( $\kappa$ -CAR/PAAm/CI<sub>1</sub>). The contact angle measurement proved that the films were hydrophobic, enhanced by increasing the CI content. The tensile strength and elongation percent values are considered adequate for materials used in wound care. The  $\kappa$ -CAR/PAAm/CI<sub>2</sub> (1.5% CI) film showed superior antimicrobial activity against *P. aeruginosa*, moderate activity against *S. aureus*, and low activity against *E. coli*. The  $\kappa$ -CAR/PAAm/CI<sub>2</sub> film effectively inhibited heat-induced hemolysis and showed wound contraction activity at a level of 100% after 19 days of excision wound treatment. The prepared films may offer a promising approach for the development of effective wound dressings.



**Citation:** Agili, F.A.; Mohamed, S.F. Synthesis and Characterization of a Self-Crosslinked Organic Copolymer Kappa-Carrageenan/Polyacrylamide/Cetrimide ( $\kappa$ -CAR/PAAm/CI) Hydrogel with Antimicrobial and Anti-Inflammatory Activities for Wound Healing. *Chemistry* **2023**, *5*, 2273–2287. <https://doi.org/10.3390/chemistry5040152>

Received: 5 October 2023

Accepted: 18 October 2023

Published: 19 October 2023



**Copyright:** © 2023 by the authors. Licensee MDPI, Basel, Switzerland. This article is an open access article distributed under the terms and conditions of the Creative Commons Attribution (CC BY) license (<https://creativecommons.org/licenses/by/4.0/>).

**Keywords:**  $\kappa$ -carrageenan; acrylamide; cetrimide; antimicrobial; anti-inflammatory; wound healing

## 1. Introduction

Wound healing criteria are affected by a variety of variables like the type of wound, the amount of fluid produced by the wound, and the patient's overall health status [1]. The use of an appropriate wound dressing is essential for preventing complications such as infection and promoting optimal wound healing [2]. Because of their excellent properties, biopolymers are extensively used as wound care materials [3]. Biopolymers can aid in the recovery process by facilitating tissue regeneration, controlling inflammation, and acting as a scaffold for cellular growth and migration [4,5]. Carrageenan,  $\alpha$ -(1–4)-3,6-anhydro-D-galactose and  $\beta$ -(1–3)-D-galactose, is a type of biopolymer derived from red seaweed that has been used in wound healing applications [6–10]. It is a polysaccharide formed from galactose and 3,6-anhydrogalactose repeating units, and its characteristics are determined by its molecular weight, degree of sulfation, and structure [11]. Carrageenan has antimicrobial properties against a variety of bacteria such as *Staphylococcus aureus* and *Pseudomonas aeruginosa*, both of which can infect wounds and slow healing [12]. However, more research is needed to fully understand its potential benefits and limitations in wound healing [13].

Polyacrylamide, poly-(2-propenamamide), is a synthetic polymer that has been used in wound healing. It promotes wound healing by creating a moist environment. The moist

environment assists in the prevention of wound desiccation, which can impede healing. Polyacrylamide protects the wound from external contaminants by maintaining the moist barrier while allowing oxygen and nutrients to reach the wound site [14–17]. It can also provide mechanical support to the wound site. The hydrogel can form a soft, conformable gel that can fill irregular wound shapes and provide a Cushing effect, which can reduce mechanical stress on the wound and minimize pain.

Cetrimide, or alkyltrimethylammonium bromide, is a quaternary ammonium compound with antiseptic properties [18]. It is commonly used as an ingredient in various pharmaceutical and personal care products [19]. Cetrimide is primarily used for its antimicrobial effects [20], helping to prevent or treat infections caused by bacteria and fungi [21].

The reaction of the sulfonic acid group ( $-\text{SO}_3\text{H}$ ) with the amide group ( $-\text{CONH}_2$ ) can lead to the formation of a sulfonamide ( $-\text{SO}_2\text{NH}-$ ) group. This reaction can occur in both organic and inorganic chemistry contexts. The resulting sulfonamide product can have a range of applications in organic synthesis, pharmaceuticals, and materials science. Sulfonamide compounds are often used as drugs for their antibacterial, antifungal, and diuretic properties [22]. It is well-known that sulfa drugs (sulfonamides) are a group of synthetic antimicrobial agents that have been widely used to treat bacterial infections. They work by inhibiting the growth and reproduction of bacteria, specifically by interfering with the biosynthesis of folic acid, which is essential for bacterial cell metabolism. Sulfonamides are bacteriostatic, meaning that they inhibit the growth of bacteria rather than directly killing them [23]. They interfere with PABA (*p*-aminobenzoic acid) in the biosynthesis of folic acid, leading to impaired DNA, RNA, and protein synthesis, and ultimately bacterial cell death.

Covalently crosslinked  $\kappa$ -carrageenan/polyacrylamide double network (DN) hydrogels were prepared using a UV initiator in the presence of KCl as an ionic charge carrier and *N,N*-methylenebisacrylamide as a crosslinker, intended to be used as self-healing materials [24,25]. Although DN hydrogels have excellent mechanical properties, most of them exhibit negligible fatigue resistance through the effect of irreversible covalent bonds [26].

Physical crosslinking methods such as ionic crosslinking represent an efficient route to prepare three-dimensional network polymers without using toxic chemical agents. The chemicals used in chemical crosslinking are often toxic, and the residual crosslinker must be removed before its use in biomedical applications [27].

In this study, a self-crosslinked  $\kappa$ -carrageenan/polyacrylamide hydrogel film was prepared successfully for the first time without using an initiator or crosslinker with the manual casting method. Cetrimide (CI) was added to the network structure to obtain a material that has dual healing and anti-inflammatory effects. The structures of the  $\kappa$ -CAR/PAAm/CI films were studied using FT-IR. The thermal and mechanical properties were investigated. Investigations of their antimicrobial, anti-inflammatory, and wound healing activities were also performed.

## 2. Materials and Methods

### 2.1. Materials

$\kappa$ -Carrageenan (Gelcarin GP 812, Irish Moss–CAS:9000-07-1) was provided by Phytotechnology laboratories, (Lenexa, KS, USA) Prod No:C257, Lot: 04F25709B, and acrylamide was obtained from Sigma (St. Louis, MO, USA). Cetrimide ( $\text{C}_{17}\text{H}_{38}\text{BrN}$ ) was provided by QualiChem's Fine Chem Pvt. Ltd., Vadodara, India (Figure 1). The utilized chemicals and reagents were high-quality and used without other purification.

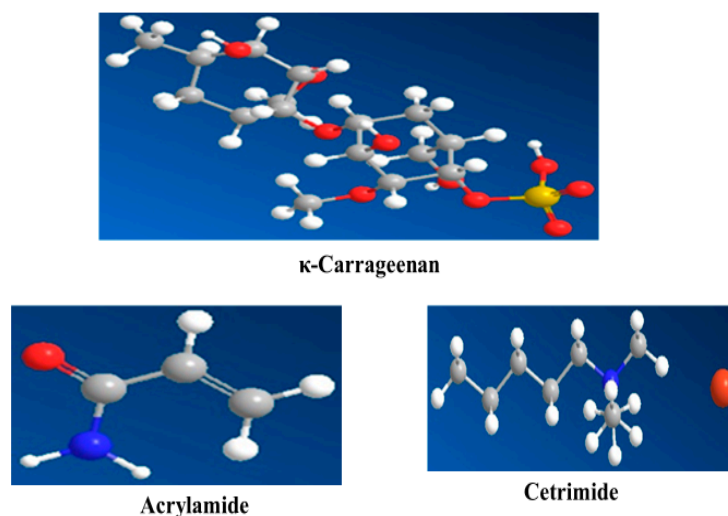


**Figure 1.** The 3D structures of  $\kappa$ -carrageenan, acrylamide, and cetrimide, respectively.

### 2.2. Preparation of $\kappa$ -CAR/PAAm/CI Films

In this study, a straightforward methodology was employed to prepare healing films based on  $\kappa$ -carrageenan/polyacrylamide (PAAm). Initially, 2 g of  $\kappa$ -Carrageenan was dissolved in 100 mL of distilled water. Once fully dissolved, 5 g of acrylamide (AAm) was added and heated to 80 °C for 2 h, resulting in a viscous solution named  $\kappa$ -CAR/PAAm. Defined amounts of  $\kappa$ -CAR/PAAm were mixed with a 1% (*w/w*) aqueous solution of cetrimide, as specified in Table 1. Subsequently, 30 wt% of glycerol was introduced into the solution through 2 h of stirring. Following this, 15 mL of the solution was poured into 10 cm Petri dishes and kept in an oven at 40 °C for 24 h. Afterward, the films were immersed in distilled water at 60 degrees Celsius for 3 h. After that, the films were washed multiple times with hot water, soaked in water for 24 h, and then dried in an oven at 60 degrees Celsius. This treatment effectively eliminated any unreacted species. Furthermore, the degree of conversion, determined according to a reference method, was measured to be  $90.1 \pm 2.3\%$ , contributing to the hydrophobic characteristics of the films [28].

**Table 1.** Composition of the CI-reinforced  $\kappa$ -CAR/PAAm films.

Code	$\kappa$ -CAR/PAAm (mL)	Cetrimide (mL)
$\kappa$ -CAR/PAAm/CI <sub>0</sub>	15.0	0.0
$\kappa$ -CAR/PAAm/CI <sub>1</sub>	14.5	0.5
$\kappa$ -CAR/PAAm/CI <sub>2</sub>	13.5	1.5

### 2.3. Fourier Transform Infrared Spectroscopy (FT-IR)

The main functional groups present in the pure  $\kappa$ -carrageenan,  $\kappa$ -CAR/PAAm/CI<sub>0</sub>, and  $\kappa$ -CAR/PAAm/CI<sub>2</sub> films were identified using FT-IR spectroscopy, performed with a Bruker Unicom infrared spectrophotometer (Rheinstetten, Germany), and the spectra were recorded within the 400–4000 cm<sup>-1</sup> wavelength region.

### 2.4. Thermal Gravimetric Analysis (TGA)

The thermal stability of the pure  $\kappa$ -CAR, CAR/PAAm/CI<sub>0</sub>,  $\kappa$ -CAR/PAAm/CI<sub>1</sub>, and  $\kappa$ -CAR/PAAm/CI<sub>2</sub> films around the sterilization temperature was investigated through thermal gravimetric analysis (TGA) using a Shimadzu TGA-30 instrument (Kyoto, Japan) in a nitrogen atmosphere. The analysis covered a temperature range from room temperature to 600 °C, with a heating rate of 10 °C/min.

### 2.5. Mechanical Properties

The mechanical properties of the  $\kappa$ -CAR/PAAm/CI<sub>0</sub> and  $\kappa$ -CAR/PAAm/CI<sub>2</sub> samples were assessed through tensile testing using Hounsfield tensile testing equipment (Haida Equipment Co. Ltd., Dongguan, China) (model H10 KS). Dumb-bell-shaped specimens measuring 50 mm in length with a 4 mm neck width were employed for the tests, which were conducted at room temperature. The stretching speed of the film was set at 10 mm/min, and a 20 kN load cell was utilized.

### 2.6. Contact Angle Measurements

The hydrophobicity or wettability of the  $\kappa$ -CAR/PAAm/CI<sub>0</sub> and  $\kappa$ -CAR/PAAm/CI<sub>2</sub> films was examined by measuring the contact angle at room temperature. A VCA Video Contact Angle System (model Krüss DSA25B, Nürnberg, Germany) was employed for this purpose. A digital micro-syringe was utilized to place a water droplet on the film surface, the film being fixed on a leveled, smooth platform [29]. To ensure accuracy, triple measurements were taken for each film at different locations.

### 2.7. Antimicrobial Activity

The antimicrobial activity of the  $\kappa$ -CAR/PAAm/CI<sub>2</sub> films was investigated using the agar well diffusion method [30]. In this approach, a microbial inoculum volume was evenly spread across the surface of an agar medium. The antimicrobial efficacy of the films was evaluated against three strains of bacteria, including one Gram-positive type, *Staphylococcus aureus* (*S. aureus*), and two Gram-negative types, *Pseudomonas aeruginosa* (*P. aeruginosa*) and *Escherichia coli* (*E. coli*). This test allowed us to assess the ability of the  $\kappa$ -CAR/PAAm/CI<sub>2</sub> films to inhibit the growth of both Gram-positive and Gram-negative bacteria, providing valuable insights into their potential as antimicrobial wound dressings.

### 2.8. Anti-Inflammatory Activity

The anti-inflammatory activity of  $\kappa$ -CAR/PAAm/CI<sub>0</sub>,  $\kappa$ -CAR/PAAm/CI<sub>1</sub>, and  $\kappa$ -CAR/PAAm/CI<sub>2</sub> was investigated using the following protocol: Fresh blood collected from healthy volunteers was placed in heparinized tubes and centrifuged at 3000 rpm for 10 min. The red blood pellets were dissolved in normal saline, and the resulting volume was measured. A 40% w/w suspension was prepared by reconstituting the dissolved red blood pellets with an isotonic buffer solution (10 mM sodium phosphate buffer, pH 7.4) containing NaH<sub>2</sub>PO<sub>4</sub>, Na<sub>2</sub>HPO<sub>4</sub>, and NaCl. The samples were dissolved in distilled water to create a hypotonic solution. Duplicate pairs of centrifuge tubes were prepared for each dose of the extract (ranging from 100 to 1000 µg/mL) in both hypotonic and isotonic solutions. Control tubes containing distilled water or 200 µg/mL of indomethacin were also prepared. To each tube, we added 0.1 mL of erythrocyte suspension, which was mixed slowly. The mixture was incubated at 37 °C for an hour and then centrifuged for 3 min at 1300 rpm. The supernatant was estimated at 540 nm using a spectrophotometer (Milton Roy, Golden, CO, USA). The hemolysis percent was calculated considering the amount of hemolysis produced in the presence of distilled water to be 100%. The hemolysis inhibition percentage of the extract was calculated accordingly:

$$\text{Inhibition of haemolysis (\%)} = 1 - \frac{OD_2 - OD_1}{OD_3 - OD_1} \times 100 \quad (1)$$

where  $OD_1$  is the absorbance of the test sample in the isotonic solution,  $OD_2$  is the absorbance of the test sample in the hypotonic solution, and  $OD_3$  is the absorbance of the control sample in the hypotonic solution.

### 2.9. In Vivo Wound Healing

#### 2.9.1. Excision Wound Mode

Animals were randomly assigned to groups for the evaluation of wound healing activity. Male mice weighing between 50 and 60 g were utilized to evaluate the effectiveness

of the biofilms  $\kappa$ -CAR/PAAm/CI<sub>0</sub> and  $\kappa$ -CAR/PAAm/CI<sub>2</sub> in wound healing through *in vivo* testing in comparison to an untreated control group. The mice received standard pellet diets and water and were kept in carefully controlled environments with 12 h light and dark cycles. The mouse's dorsal fur was shaved with an electric trimmer, and a wound with a diameter and depth of 100 mm<sup>2</sup> and 1 mm was made with sterilized surgical scissors. Biofilms of 1.5 cm × 1.5 cm sheets were applied to the wounded areas. Wound healing progress was evaluated using naked eye observation of the wound's contraction, epithelialization, and wound morphology. Photographs were taken at each measurement interval [31].

### 2.9.2. Measurement of Wound Contraction

Wound size was measured immediately and on the 7th, 14th, and 21st days post-operation. The evaluation of wound healing was performed using 12 mice, divided equally into three groups. The first group was used as a control, with shaving alone and no dressing. The second group was treated with  $\kappa$ -CAR/PAAm/CI<sub>0</sub> films, while the third group was treated with  $\kappa$ -CAR/PAAm/CI<sub>2</sub> films. The evaluated surface area was used to calculate the percentage of wound contraction, taking the initial size of the wound (100 mm<sup>2</sup>) as 100% as in the following Equation:

$$\text{Percentage of wound reduction \%} = \frac{\text{Initial wound area} - \text{wound area after a time intervals}}{\text{Initial wound area}} \times 100 \quad (2)$$

### 2.10. Statistical Analysis

All results were statistically analyzed using one-way ANOVA. Differences among average values were analyzed with Duncan's multiple range test using IBM SPSS software version 24 as a statistical resource at  $p < 0.05$ .

## 3. Results and Discussion

### 3.1. Synthetic Route of $\kappa$ -CAR/PAAm/CI Films

A  $\kappa$ -CAR/PAAm double-network hydrogel system was effectively produced due to its distinctive properties [32]. Yu et al. prepared the system using Zr<sup>4+</sup> ions to crosslink the first network under UV irradiation in the presence of an  $\alpha$ -ketoglutaric acid photoinitiator and *N,N'*-methylene bis-acrylamide crosslinker [33]. Deng et al. prepared the system using K<sup>+</sup> ions to crosslink the first network and an ammonium persulfate initiator [34]. In this study,  $\kappa$ -CAR/PAAm was prepared through a physical crosslinking method without using any initiator or crosslinker. When mixing carrageenan with acrylamide and heating the solution to 80 degrees Celsius, the thermal energy provided by the elevated temperature may be sufficient to initiate the polymerization of acrylamide without the need for a chemical initiator, as described in previous studies [35–37]. At 80 degrees Celsius, the acrylamide monomer can diffuse into the carrageenan solution and react with the carrageenan chains to form a copolymer. The carrageenan chains in the copolymer may be crosslinked with each other through the AAm. After casting and cooling, the carrageenan–acrylamide copolymer may be highly entangled, making it difficult for water molecules to penetrate the film. To ensure that no residue of AAm monomer remained in the copolymer matrix, the films were soaked for three hours in water at 60 °C, washed many times, and soaked overnight in water. Figure 2 shows the possible synthesis route for  $\kappa$ -CAR/PAAm/CI through the formation of a sulfonamide linkage and Michael addition between CAR and AAm. The same mechanism was reported in the polymerization route of chitosan/acrylic acid copolymer [27]. Moreover, cetrimide was linked with  $\kappa$ -CAR through electrostatic interaction between the positively charged amino group of cetrimide and the negatively charged sulfate group of  $\kappa$ -CAR. This mechanism is consistent with that previously explained by Cao et al., who synthesized complex hydrogel beads composed of hydrolyzed polyacrylamide (HPAM) and chitosan through an electrostatic interaction [28]. Moreover, the chitosan/ $\kappa$ -carrageenan hydrogel was greenly prepared through an electrostatic interaction between positively charged amino

groups on chitosan with negatively charged sulfate groups on  $\kappa$ -CAR without any toxic agent [38].

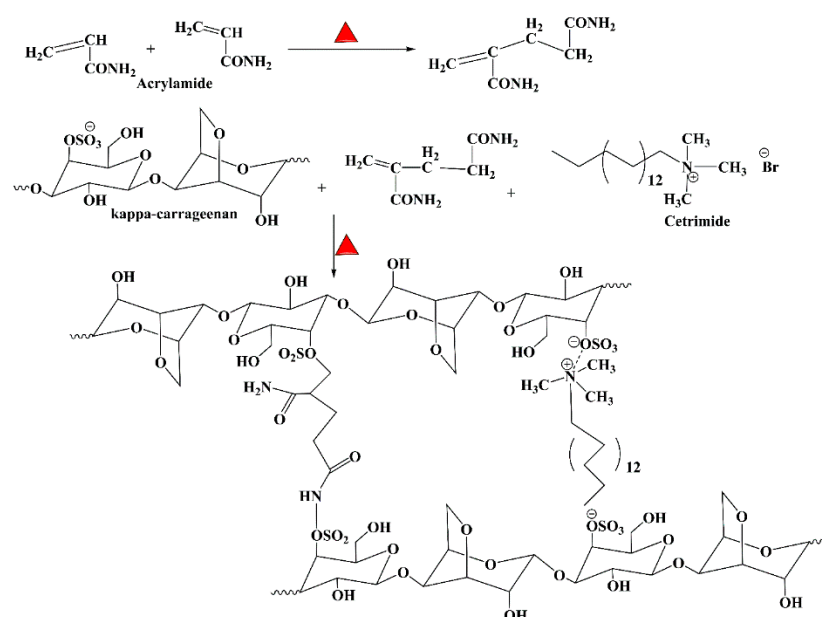


**Figure 2.** The synthesis route for  $\kappa$ -CAR/PAAm/CI preparation. Red triangle is the symbol of heating.

### 3.2. Spectral Analysis

The FT-IR spectrum of the pure  $\kappa$ -carrageenan exhibited characteristic absorption peaks that included  $-\text{OH}$  stretching vibration at  $3280\text{ cm}^{-1}$ ,  $-\text{CH}$  at  $2920\text{ cm}^{-1}$ , the polymer-bound water at  $1624\text{ cm}^{-1}$ ,  $\text{O}=\text{S}=\text{O}$  at  $1237\text{ cm}^{-1}$ , glycoside bond at  $1044\text{ cm}^{-1}$ , ether group in the 3,6-anhydrogalactose of the carrageenan at  $918\text{ cm}^{-1}$ , and sulfate ester bonding in galactose at  $849\text{ cm}^{-1}$  (Figure 3) [39]. The FT-IR spectrum of the pure AAm features a prominent strong peak at  $1613\text{ cm}^{-1}$ , attributed to the vibration of  $\text{C}=\text{C}$  in pure AAm. Additionally, the hydrogen (H) peaks associated with the  $\text{C}=\text{C}-\text{H}$  bonds at approximately  $980\text{ cm}^{-1}$ , which are clear in pure AAm, exhibited reduced intensity. The FT-IR spectra of both  $\kappa$ -CAR/PAAm/CI<sub>0</sub> and  $\kappa$ -CAR/PAAm/CI<sub>2</sub> are shown in Figure 3. Remarkably, the  $\text{C}=\text{C}$  peak at  $1613\text{ cm}^{-1}$ , indicative of AAm, is conspicuously absent in these spectra, strongly suggesting that the acrylamide (AAm) underwent full and successful polymerization into polyacrylamide (PAAm) in these samples. The FT-IR spectrum of  $\kappa$ -CAR/PAAm/CI<sub>0</sub> showed a broad band of  $-\text{OH}$  centered at  $3370\text{ cm}^{-1}$ . It must be noted that the splitting of the  $-\text{OH}$  group may reflect the presence of two different types of hydrogen bonds: intramolecular and intermolecular hydrogen bonds [40]. Another reason for this splitting may correspond to the hydrogen bonded OH group and the non-hydrogen bonded OH group. The band of  $\text{C}=\text{O}$  of the amide group appears at  $1672\text{ cm}^{-1}$  [41]. The peaks at  $1222$  and  $1040\text{ cm}^{-1}$  are due to the sulfate group stretching vibrations and the anhydrogalactose unit in CAR, respectively. The pyranose ring peak appears at  $603\text{ cm}^{-1}$ . The effect of CI on the chemical structure of  $\kappa$ -CAR/PAAm/CI<sub>2</sub> was obtained, as shown in Figure 3. A slight change in the spectrum of  $\kappa$ -CAR/PAAm/CI<sub>2</sub> when compared to  $\kappa$ -CAR/PAAm/CI<sub>0</sub> indicated that there is no significant chemical interaction between CI and  $\kappa$ -CAR/PAAm. The peaks of the sulfate group, the anhydrogalactose unit, and pyranose ring stretching vibrations in  $\kappa$ -CAR were affected, which reflected the rearrangement of these groups through the effect of CI.

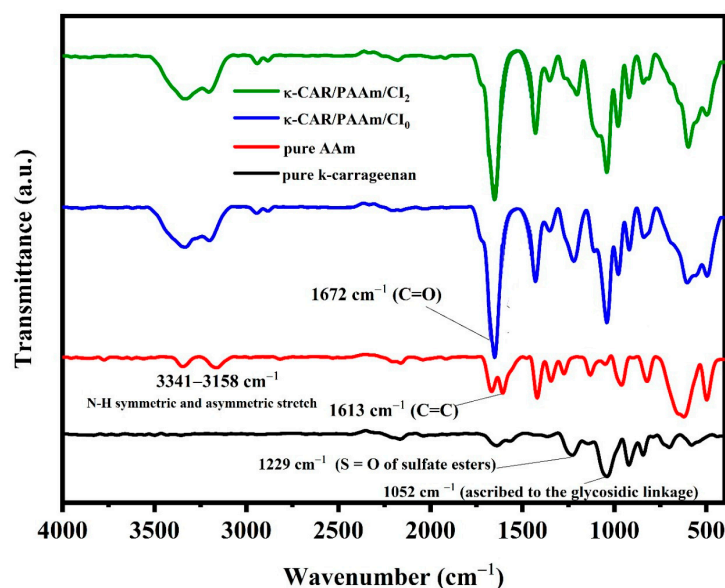


**Figure 3.** FT-IR spectra of pure  $\kappa$ -CAR, pure AAm,  $\kappa$ -CAR/PAAm/Cl<sub>0</sub>, and  $\kappa$ -CAR/PAAm/Cl<sub>2</sub> films.

### 3.3. Thermogravimetric Analysis (TGA)

TGA and DTA thermograms of the pure  $\kappa$ -CAR,  $\kappa$ -CAR/PAAm/Cl<sub>0</sub>,  $\kappa$ -CAR/PAAm/Cl<sub>1</sub>, and  $\kappa$ -CAR/PAAm/Cl<sub>2</sub> are shown in Figure 4. For the pure  $\kappa$ -CAR, the first stage of decomposition occurred at 120 °C due to the loss of water and other volatile compounds. The main degradation of  $\kappa$ -CAR occurred in the range of 250 °C, where a rapid weight loss was observed, indicating the decomposition of the polysaccharide backbone [42]. In light of the results obtained in our study, it is evident that  $\kappa$ -CAR possesses impressive thermal stability characteristics, making it a valuable material for various industrial and food-related applications [43]. It can be observed that the thermogram of  $\kappa$ -CAR/PAAm/Cl<sub>0</sub> has three decomposition stages. The first stage occurred at around 100 °C, where a small amount of weight was lost owing to the loss of physically adsorbed water. The second stage, occurring at 186 °C, may be attributed to the elimination of the  $-\text{OSO}_3^-$  and  $-\text{NH}_2$  side groups and the carbohydrate backbone's fragmentation. The third stage occurred at 330 °C due to the further decomposition of the backbone carbon chains. The charred residue of  $\kappa$ -CAR/PAAm/Cl<sub>0</sub> is much less than that of pure  $\kappa$ -CAR, which explains the high level of crosslink formation between  $\kappa$ -CAR and AAm. It can be noted that a decrease in thermal stability was obtained with the incorporation of Cl into  $\kappa$ -CAR/PAAm/Cl<sub>1</sub>. The first stage occurred at 133 °C, and the second and third stages occurred at 220 °C and 392 °C. An improvement in the thermal stability of  $\kappa$ -CAR/PAAm/Cl<sub>2</sub> was obtained, as compared to  $\kappa$ -CAR/PAAm/Cl<sub>1</sub>. The first stage occurred at 112 °C, and the second and third stages occurred at 231 °C and 421 °C.

### 3.4. Contact Angle

The water contact angle for  $\kappa$ -CAR/PAAm/Cl<sub>0</sub>,  $\kappa$ -CAR/PAAm/Cl<sub>1</sub>, and  $\kappa$ -CAR/PAAm/Cl<sub>2</sub> was measured as seen in Figure 5. The contact angle of  $\kappa$ -CAR/PAAm/Cl<sub>0</sub> is 117.95°, indicating that the  $\kappa$ -CAR/PAAm/Cl<sub>0</sub> is hydrophobic. It must be pointed out that  $\kappa$ -CAR and AAm are hydrophilic materials; however, the  $\kappa$ -CAR/PAAm/Cl<sub>0</sub> substrate prevents water from spreading or wetting the surface. This confirmed the unique structural and chemical properties of  $\kappa$ -CAR/PAAm/Cl<sub>0</sub>. The excessive chemical and physical bonds which are formed create a more highly crosslinked structure. This structure may create a hydrophobic barrier that prevents water or other liquids from penetrating the  $\kappa$ -CAR/PAAm/Cl<sub>0</sub> film. It can be also noted that the contact angles of  $\kappa$ -CAR/PAAm/Cl<sub>1</sub> and  $\kappa$ -CAR/PAAm/Cl<sub>2</sub> are 126.60° and 139.30° due to the increasing hydrophobicity as

a result of including CI in the film substrate. The same angle was obtained for an alkali cellulose/polyvinyl alcohol biofilm [44].

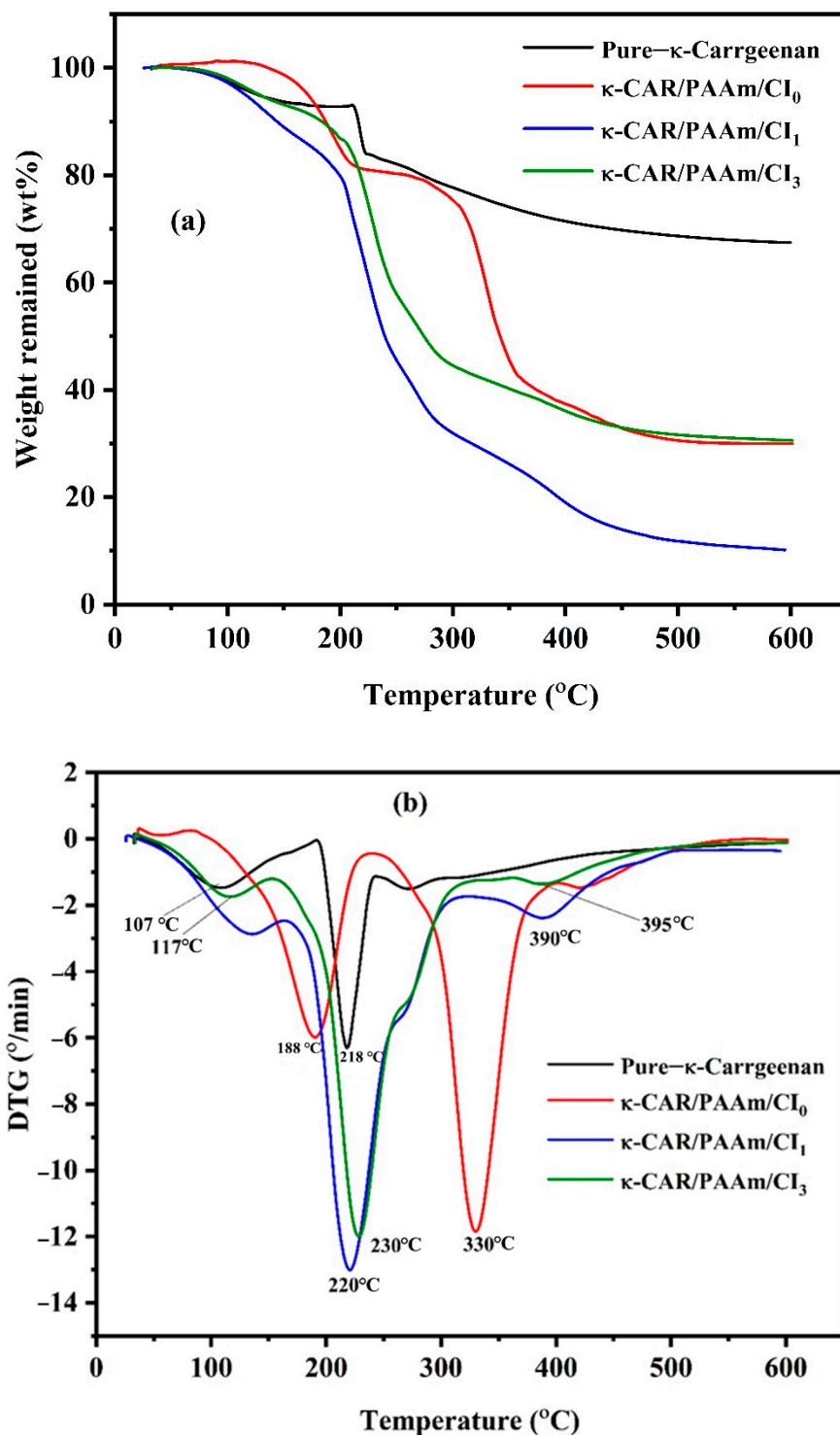
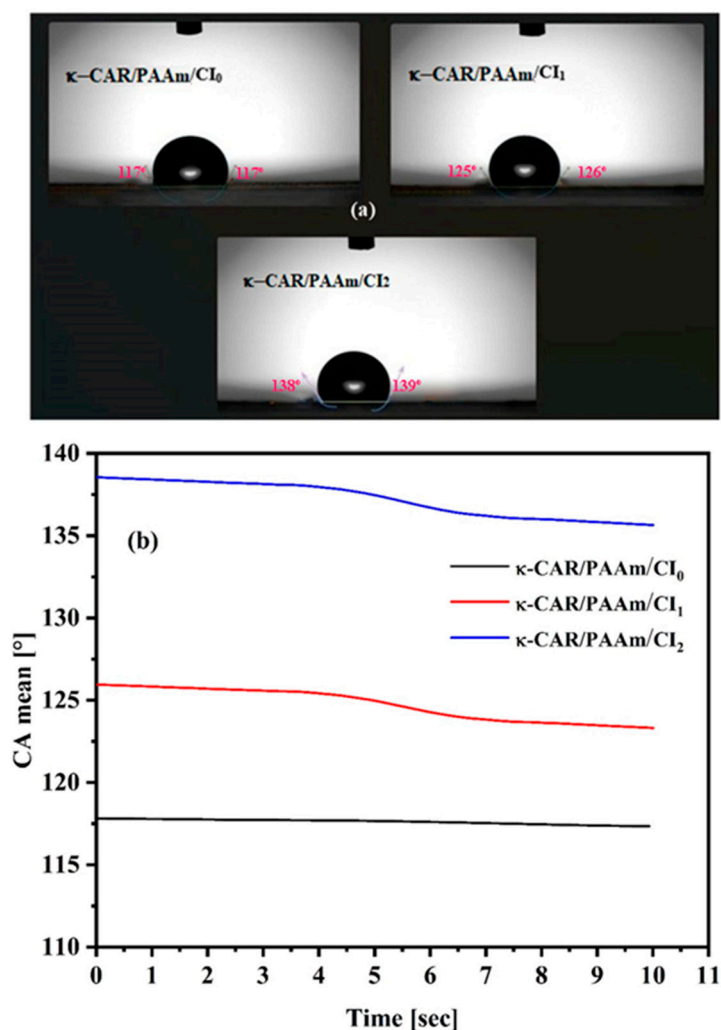


Figure 4. TGA (a) and DTA (b) thermograms of pure κ-CAR κ-CAR/PAAm/CI<sub>0</sub>, κ-CAR/PAAm/CI<sub>1</sub>, and κ-CAR/PAAm/CI<sub>2</sub> films.



**Figure 5.** The contact angles (a) and the time-dependent change (b) of the water contact angle for  $\kappa\text{-CAR/PAAm/CI}_0$ ,  $\kappa\text{-CAR/PAAm/CI}_1$ , and  $\kappa\text{-CAR/PAAm/CI}_2$  films.

The increased hydrophobicity of the prepared  $\kappa\text{-CAR/PAAm/CI}_0$  films after the addition of cetrimide ( $\kappa\text{-CAR/PAAm/CI}_1$  and  $\kappa\text{-CAR/PAAm/CI}_2$  films), as indicated by the contact angle results, is a key characteristic essential for their role as wound dressings. This controlled hydrophobicity serves multiple purposes, including effective exudate management to maintain an optimal wound healing environment, the prevention of dressing dissolution upon contact with moisture or bodily fluids, and the provision of water-resistant qualities. The level of hydrophobicity is carefully controlled during the film preparation process to strike the right balance between moisture management and patient comfort, ensuring the films' durability and effectiveness in managing wound exudates without dissolution, making them well-suited for their intended application as wound dressings.

### 3.5. Mechanical Properties

The mechanical properties of the  $\kappa\text{-CAR/PAAm/CI}_2$  film were thoroughly examined and compared with those of the  $\kappa\text{-CAR/PAAm/CI}_0$  film, as visually depicted in Figure 6a–c. The mechanical characteristics of wound dressings are of paramount importance due to their direct influence on wound healing outcomes. Among these properties, a high tensile strength and Young's modulus (MPa) are particularly desirable, as they confer robustness and durability to the film. Notably,  $\kappa\text{-CAR/PAAm/CI}_2$  displayed a significantly higher Young's modulus (MPa) of 25.47 MPa, while  $\kappa\text{-CAR/PAAm/CI}_0$  registered at 16.45 MPa. This discrepancy underscores the pivotal role of CI in enhancing the crosslink-

ing and mechanical strength of  $\kappa$ -CAR/PAAm/Cl<sub>2</sub>. Conversely, the  $\kappa$ -CAR/PAAm/Cl<sub>2</sub> film exhibited a percentage of elongation at a break of 15.89%, a measure of flexibility. It is crucial to recognize that the specific wound type and stage of healing can influence the ideal mechanical properties of wound dressings, and a 15.89% elongation at break may be considered suitable for wound healing and various applications in the field of wound care. These mechanical properties are vital in tailoring wound dressings to balance protection, comfort, and wound healing requirements, emphasizing the material's suitability for various wound care applications.

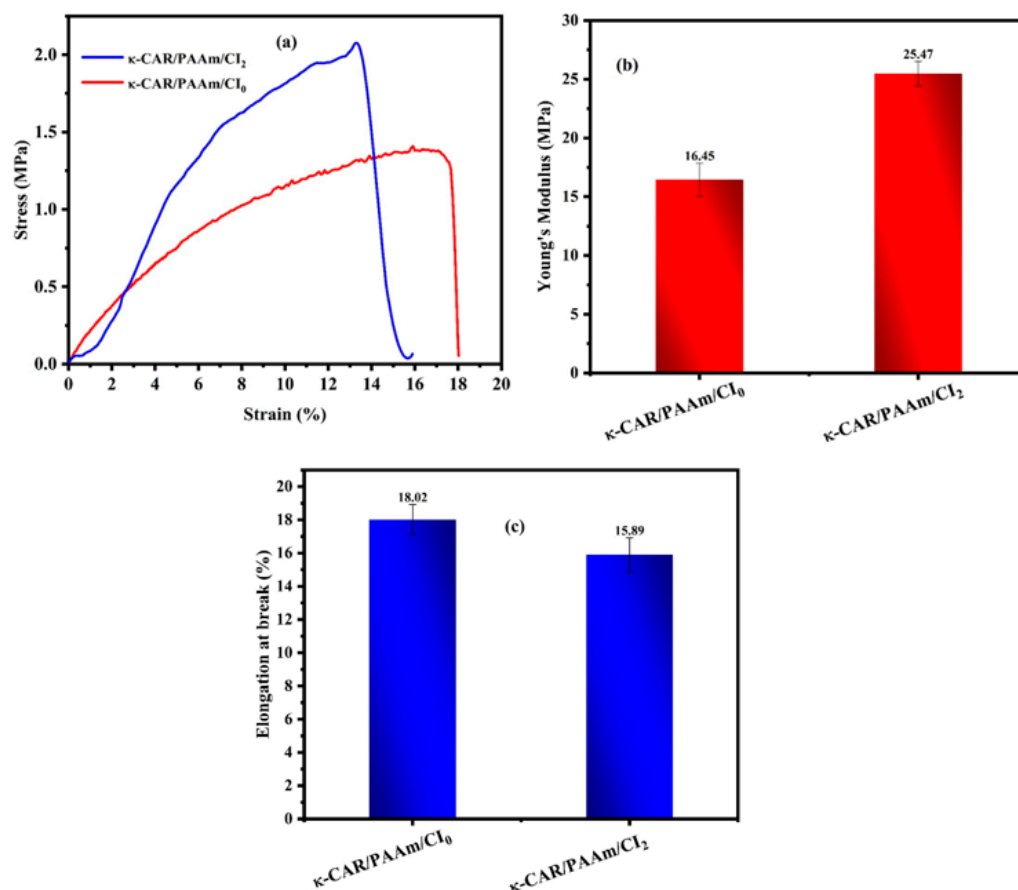


**Figure 6.** The mechanical properties of  $\kappa$ -CAR/PAAm/Cl<sub>0</sub> and  $\kappa$ -CAR/PAAm/Cl<sub>2</sub> films: (a) stress/strain, (b) Young's modulus (MPa), and (c) elongation at break (%).

### 3.6. Antimicrobial Activity

The antimicrobial activity of the  $\kappa$ -CAR/PAAm/Cl<sub>2</sub> films against *Staphylococcus aureus* (*S. aureus*), a Gram-positive bacteria, and *Pseudomonas aeruginosa* (*P. aeruginosa*) and *Escherichia coli* (*E. coli*), Gram-negative bacteria, was studied, as shown in Figure 7. It is clear that the  $\kappa$ -CAR/PAAm/Cl<sub>2</sub> films showed potent antibacterial properties against the investigated pathogens. The inhibition zones of *S. aureus*, *P. aeruginosa*, and *E. coli* were found to be 15, 31, and 13 mm, respectively. This means the  $\kappa$ -CAR/PAAm/Cl<sub>2</sub> films have superior antimicrobial activity against *P. aeruginosa* and moderate antimicrobial activity against *S. aureus*, while they have low antimicrobial activity against *E. coli*. The results of the present study are consistent with the literature. The results regarding the antibacterial properties of the  $\kappa$ -CAR/PAAm/Cl<sub>2</sub> films showed considerable antimicrobial activity. This remarkable antibacterial performance can be attributed, in part, to the properties of cetrimide (CI), which serves as an essential component of the film's formulation. Cetrimide is known for its inherent antimicrobial activity and has been widely utilized for its ability to inhibit the growth of both Gram-positive and Gram-negative bacteria [45]. The

antimicrobial mechanism of cetrimide often involves disrupting the integrity of bacterial cell membranes, thereby compromising their structural and functional integrity. The incorporation of CI into  $\kappa$ -CAR/PAAm films likely enhances their antimicrobial efficacy, making them promising candidates for applications where infection control and wound protection are critical.

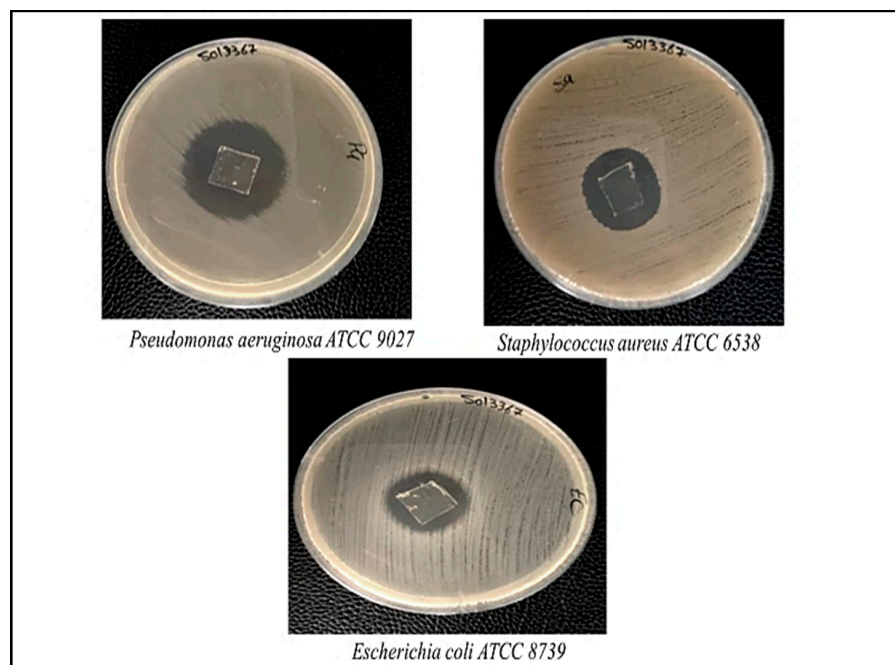


**Figure 7.** Antimicrobial activity of  $\kappa$ -CAR/PAAm/CI<sub>2</sub> films.

### 3.7. Anti-Inflammatory Activity

The anti-inflammatory activity of the  $\kappa$ -CAR/PAAm/CI<sub>0</sub>,  $\kappa$ -CAR/PAAm/CI<sub>1</sub>, and  $\kappa$ -CAR/PAAm/CI<sub>2</sub> films were investigated, as shown in Figure 8. The hemolysis curve shows that the hemolysis assay yielded good results and met our expectations. The hemolysis inhibition percent at a concentration 1000  $\mu$ g/mL was found to be 97.9, 70.7, and 65.4% for the  $\kappa$ -CAR/PAAm/CI<sub>2</sub>,  $\kappa$ -CAR/PAAm/CI<sub>1</sub>, and  $\kappa$ -CAR/PAAm/CI<sub>0</sub> films, respectively. It can be observed that the  $\kappa$ -CAR/PAAm/CI<sub>2</sub> film exhibited the highest edema inhibition percent, followed by  $\kappa$ -CAR/PAAm/CI<sub>1</sub>, and the lowest one was the  $\kappa$ -CAR/PAAm/CI<sub>0</sub> film. It must be noted that the  $\kappa$ -CAR/PAAm/CI<sub>2</sub> film effectively inhibited heat-induced hemolysis [46].

### 3.8. Wound Healing Activity of the Films

The wound contraction reflects the wound healing progress on the 7th, 14th, and 21st days, comparing the groups treated with the  $\kappa$ -CAR/PAAm/CI<sub>0</sub> and  $\kappa$ -CAR/PAAm/CI<sub>2</sub> films to an untreated control (Table 2, Figure 9). The results obtained reveal a significant enhancement in wound closure. After 7 days of treatment, the wound closure percentages were 71%, 53%, and 51% for the groups treated with  $\kappa$ -CAR/PAAm/CI<sub>2</sub> and  $\kappa$ -CAR/PAAm/CI<sub>0</sub> and the untreated control, respectively. By day 14, the wound closure percentages had improved to 98%, 90%, and 73% for the groups treated with  $\kappa$ -CAR/PAAm/CI<sub>2</sub> and  $\kappa$ -CAR/PAAm/CI<sub>0</sub> and the untreated control, respectively. Impressively, on day 21, the groups treated with the  $\kappa$ -CAR/PAAm/CI<sub>2</sub> and  $\kappa$ -CAR/PAAm/CI<sub>0</sub> films exhibited rapid healing, achieving nearly 100% wound closure, while the untreated control reached 82%. These results underscore the substantial reduction in the wound area facilitated by the  $\kappa$ -CAR/PAAm/CI<sub>2</sub> film. The incorporation of cetrimide improved the film potential to expedite wound healing and shorten the epithelialization period to 19 days and 22 days in the groups treated with the  $\kappa$ -CAR/PAAm/CI<sub>2</sub> and  $\kappa$ -CAR/PAAm/CI<sub>0</sub>

films, respectively, while in the control group, it was 26 days. The presence of  $\kappa$ -CAR in the film, with its sulfur groups, may contribute to this effect by promoting keratosis and histological changes and offering immunomodulatory properties [47].

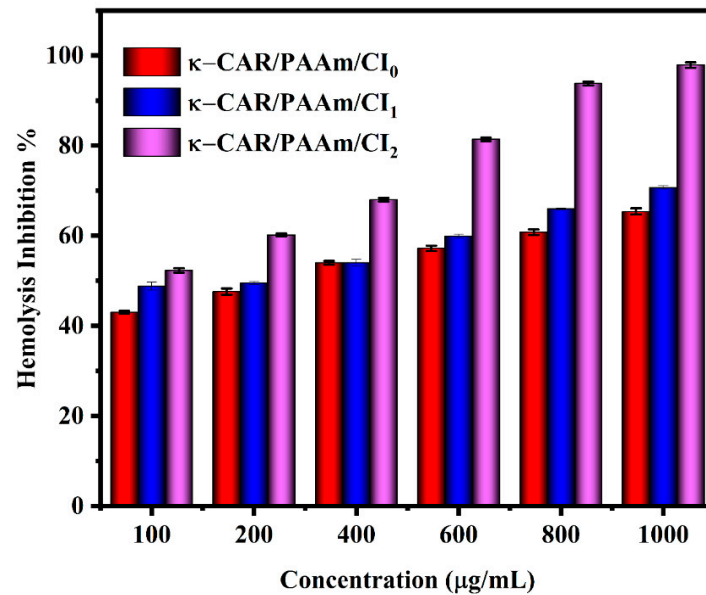


Figure 8. Anti-inflammatory activity graph of  $\kappa$ -CAR/PAAm/CI<sub>0</sub>,  $\kappa$ -CAR/PAAm/CI<sub>1</sub>, and  $\kappa$ -CAR/PAAm/CI<sub>2</sub> films.

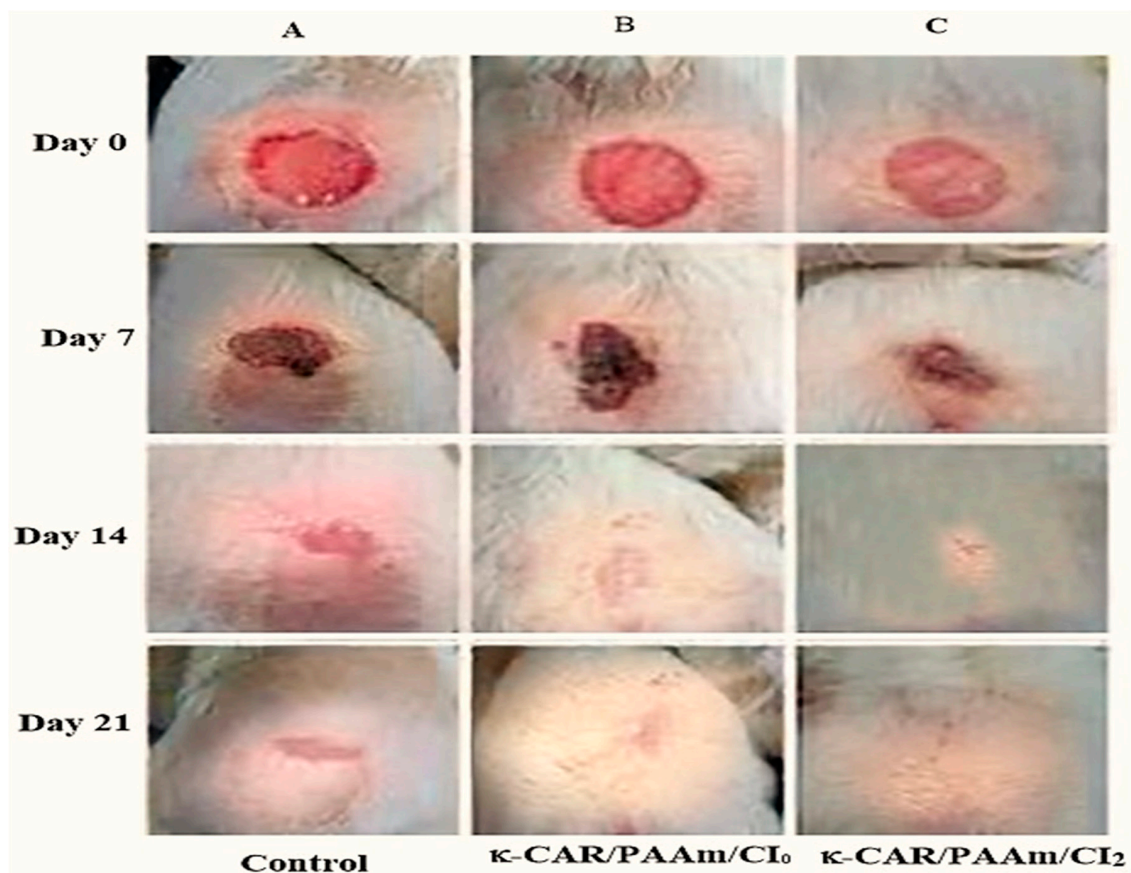


Figure 9. Wound healing appearance during 21-day study period in different treatment groups: (A) control untreated, (B) treated with  $\kappa$ -CAR/PAAm/CI<sub>0</sub>, and (C) treated with  $\kappa$ -CAR/PAAm/CI<sub>2</sub> films.

**Table 2.** Effect of  $\kappa$ -CAR/PAAm/CI<sub>0</sub> and  $\kappa$ -CAR/PAAm/CI<sub>2</sub> films on excision wound contraction.

Group (Treatment)	Wound Area (mm <sup>2</sup> ) on Post-Wounding Days					
	Day 7		Day 14		Day 21	
	Wound Area (mm <sup>2</sup> )	% Wound Contraction *	Wound Area (mm <sup>2</sup> )	% Wound Contraction *	Wound Area (mm <sup>2</sup> )	% Wound Contraction *
Control	49 ± 2.4	51	27 ± 1.3	73	18 ± 0.1	82
Treated with $\kappa$ -CAR/PAAm/CI <sub>0</sub>	47 ± 1.6	53	10 ± 2.06	90	3 ± 0.31	97
Treated with $\kappa$ -CAR/PAAm/CI <sub>2</sub>	29 ± 2.7	71	2 ± 1.11	98	0	100

Notes: Wound areas are expressed as mean ± SEM (n = 4). \* % wound contraction is from the initial wound area (100 mm<sup>2</sup>).

#### 4. Conclusions

In this study, a  $\kappa$ -carrageenan/polyacrylamide/cetrimide ( $\kappa$ -CAR/PAAm/CI) film was prepared successfully for the first time without using an initiator or crosslinkers with the manual casting method. The properties of the  $\kappa$ -CAR/PAAm/CI films were studied in order to determine their applicability for use as wound healing materials. An improvement in the thermal stability of the  $\kappa$ -CAR/PAAm/CI<sub>2</sub> (CI: 1.5%) film was achieved, compared to  $\kappa$ -CAR/PAAm/CI<sub>1</sub> (CI: 0.5%). It was found that the  $\kappa$ -CAR/PAAm/CI<sub>0</sub> film is hydrophobic, where the contact angle is 117.95°. The contact angle increased to 126.60° and 139.30° for  $\kappa$ -CAR/PAAm/CI<sub>1</sub> and  $\kappa$ -CAR/PAAm/CI<sub>2</sub>, respectively, through the effect of CI. The tensile strength and elongation percent values are considered adequate for materials used in wound care. The  $\kappa$ -CAR/PAAm/CI<sub>2</sub> film showed antibacterial activity against *S. aureus*, *P. aeruginosa*, and *E. coli*. The hemolysis inhibition percent at a concentration of 1000 µg/mL was found to be 97.9, 70.7, and 65.4% for the  $\kappa$ -CAR/PAAm/CI<sub>2</sub>,  $\kappa$ -CAR/PAAm/CI<sub>1</sub>, and  $\kappa$ -CAR/PAAm/CI<sub>0</sub> films, respectively. The in vivo wound healing study indicated that the incorporation of cetrimide into a  $\kappa$ -CAR/PAAm film has a beneficial impact on the wound healing process and may offer a promising approach for the development of effective wound dressings. The  $\kappa$ -CAR/PAAm/CI<sub>2</sub> film showed higher healing activity with a wound contraction percentage of 98% after 14 days of wound treatment.

**Author Contributions:** Conceptualization, F.A.A. and S.F.M.; methodology, F.A.A. and S.F.M.; investigation, F.A.A. and S.F.M.; writing—original draft preparation, S.F.M.; writing—review and editing, F.A.A.; supervision, F.A.A.; project administration, F.A.A.; funding acquisition, F.A.A. All authors have read and agreed to the published version of the manuscript.

**Funding:** This research was supported by the Deanship of Scientific Research, Jazan University, Saudi Arabia, project No. RUP3-4.

**Data Availability Statement:** All data for this research are presented in this paper.

**Acknowledgments:** The authors express their appreciation to the Deanship of Scientific Research, Jazan University, Saudi Arabia, supporting the project number RUP3-4.

**Conflicts of Interest:** The authors declare no conflict of interest.

#### References

- Han, G.; Ceilley, R. Chronic wound healing: A review of current management and treatments. *Adv. Ther.* **2017**, *34*, 599–610. [CrossRef]
- Stan, D.; Marioara, A.; Roxana, A.; Nicolae-Bogdan, M.; Andreea, L.M.; Dana, S. Wound healing applications of creams and “smart” hydrogels. *Exp. Dermatol.* **2021**, *30*, 1218–1232. [CrossRef]
- Sahana, T.; Rekha, P. Biopolymers: Applications in wound healing and skin tissue engineering. *Mol. Biol. Rep.* **2018**, *45*, 2857–2867. [CrossRef]
- Nosrati, H.; Mohammad, K.; Zohreh, A.; Mehdi, B. Cationic, anionic and neutral polysaccharides for skin tissue engineering and wound healing applications. *Int. J. Biol. Macromol.* **2021**, *192*, 298–322. [CrossRef]

5. Riha, S.M.; Maarof, M.; Fauzi, M.B. Synergistic effect of biomaterial and stem cell for skin tissue engineering in cutaneous wound healing: A concise review. *Polymers* **2021**, *13*, 1546–1574. [[CrossRef](#)]
6. Yegappan, R.; Vignesh, S.; Sivashanmugam, A.; Jayakumar, R. Carrageenan based hydrogels for drug delivery, tissue engineering and wound healing. *Carbohydr. Polym.* **2018**, *198*, 385–400. [[CrossRef](#)] [[PubMed](#)]
7. Santosh, S.B.; Pallavi, V.M.; Kaustubh, C.P.; Rohan, C.; Prachi, B.; Prajakta, D.; Ravindra, V.A. Cytotoxicity and hemostatic activity of chitosan/carrageenan composite wound healing dressing for traumatic hemorrhage. *Carbohydr. Polym.* **2020**, *239*, 116106.
8. Neamtu, B.; Andreea, B.; Mihai, O.; Cristian, S.; Dragos, P.; Marius, Z.; Vioara, M. Carrageenan-Based Compounds as Wound Healing Materials. *Int. J. Mol. Sci.* **2022**, *23*, 9117–9137. [[CrossRef](#)]
9. Mokhtari, H.; Shima, T.; Fereshteh, S.; Mahshid, K.; Hamid, R.; Seeram, R.; Filippo, B. Recent advances in chemically-modified and hybrid carrageenan-based platforms for drug delivery, wound healing, and tissue engineering. *Polymers* **2021**, *13*, 1744–1765. [[CrossRef](#)] [[PubMed](#)]
10. Natalia, P.; Saddys, R.; Rebeca, B.; Luis, B.; Sandra, F.; Francisca, L. Carrageenan-based physically crosslinked injectable hydrogel for wound healing and tissue repairing applications. *Int. J. Pharm.* **2020**, *589*, 119828.
11. Chauhan, P.S.; Saxena, A. Bacterial carrageenases: An overview of production and biotechnological applications. *Biotech* **2016**, *6*, 146–164. [[CrossRef](#)] [[PubMed](#)]
12. Jessie, L.; Rashin, N.; Slawomir, D.; Kazimiera, A.; Cyrille, B.; Edgar, H.; Bronwyn, H.; Marta, K.; David, A. Incorporation and antimicrobial activity of nisin Z within carrageenan/chitosan multilayers. *Sci. Rep.* **2021**, *11*, 1690.
13. Pereira, L. Seaweeds as source of bioactive substances and skin care therapy-cosmeceuticals, algotherapy, and thalassotherapy. *Cosmetics* **2018**, *5*, 68. [[CrossRef](#)]
14. Meng, W.; Huihua, H.; Xiaofeng, M.; Chaokang, H.; Xiaohong, P. Copper metal-organic framework embedded carboxymethyl chitosan-g-glutathione/polyacrylamide hydrogels for killing bacteria and promoting wound healing. *Int. J. Biol. Macromol.* **2021**, *187*, 699–709.
15. Zhongxiang, B.; Weihua, D.; Guofei, Y.; Yanjun, W.; Yining, C.; Yanping, H.; Changkai, Y.; Nianhua, D. Tough and tissue-adhesive polyacrylamide/collagen hydrogel with dopamine-grafted oxidized sodium alginate as crosslinker for cutaneous wound healing. *RSC Adv.* **2018**, *8*, 42123–42132.
16. Lanlan, W.; Jinhua, D.; Ziqiang, Z.; Dawei, L.; Wenhao, D.; Yingke, L.; Bingqi, J.; Haoxuan, L.; Qingsheng, L.; Bingyao, D. Quarternized chitosan/queretin/polyacrylamide semi-interpenetrating network hydrogel with recoverability, toughness and antibacterial properties for wound healing. *Int. J. Biol. Macromol.* **2023**, *228*, 48–58.
17. Gupta, A.; Marek, K.; Wayne, H.; Stephen, T.B.; Claire, M.; Iza, R. The production and application of hydrogels for wound management: A review. *Eur. Polym. J.* **2019**, *111*, 134–151. [[CrossRef](#)]
18. Grunlan, J.; Choi, J.; Lin, A. Antimicrobial behavior of polyelectrolyte multilayer films containing cetrimide and silver. *Biomacromolecules* **2005**, *6*, 1149–1153. [[CrossRef](#)] [[PubMed](#)]
19. Marto, J.; Pinto, P.; Fitas, M.; Gonçalves, L.M.; Almeida, A.J.; Ribeiro, H.M. Safety assessment of starch-based personal care products: Nanocapsules and pickering emulsions. *Toxicol. Appl. Pharmacol.* **2018**, *342*, 14–21. [[CrossRef](#)] [[PubMed](#)]
20. Mishra, A.; Pandey, R.; Manickam, N. Antibacterial effect and physical properties of chitosan and chlorhexidine-cetrimide-modified glass ionomer cements. *J. Indian Soc. Pedod. Prev. Dent.* **2017**, *35*, 28–33. [[PubMed](#)]
21. Giorgi, G.M.; Natalia, C.M.; Diana, R.P.; Augusto, E.J.; Giovanna, R.D.; Carlos, E.; Sérgio, L.P. Effect of cetrimide 2% with and without photodynamic therapy to reduce *Streptococcus mutans* burden in dentinal carious lesions. *Lasers Med. Sci.* **2021**, *36*, 1935–1940.
22. Aben, O.; Jhimli, B. Sulfonamide drugs: Structure, antibacterial property, toxicity, and biophysical interactions. *Biophys. Rev.* **2021**, *13*, 259–272.
23. Bendjeddou, A.; Abbaz, T.; Khacha, N.; Benahmed, M.; Gouasmia, A.; Villemin, D. Antibacterial activity of sulfonamide derivatives against clinical strains of bacteria. *Res. J. Pharm. Biol. Chem. Sci.* **2016**, *7*, 799–804.
24. Liu, S.; Li, L. Recoverable and self-healing double network hydrogel based on  $\kappa$ -carrageenan. *ACS Appl. Mater. Interfaces* **2016**, *8*, 29749–29758. [[CrossRef](#)]
25. Jin, W.; Zixuan, W.; Huihua, X.; Qian, W.; Chuan, L.; Bo-Ru, Y.; Xuchun, G.; Xi, X.; Kai, T.; Yi, S.; et al. An intrinsically stretchable humidity sensor based on anti-drying, self-healing and transparent organohydrogels. *Mater. Horiz.* **2019**, *6*, 595–603.
26. Linjie, Z.; Xinjie, P.; Kun, F.; Rui, Z.; Jun, F. Super tough, ultra-stretchable, and fast recoverable double network hydrogels physically crosslinked by triple non-covalent interactions. *Polymer* **2020**, *192*, 122319.
27. Baoxiao, C.; Boying, P.; Zhengke, W.; Qiaoling, H. Advances in chitosan-based superabsorbent hydrogels. *RSC Adv.* **2017**, *7*, 42036–42046.
28. Jie, C.; Yebang, T.; Yuju, C.; Qiang, M. Fabrication and properties of superabsorbent complex gel beads composed of hydrolyzed polyacrylamide and chitosan. *J. Appl. Polym. Sci.* **2010**, *116*, 3338–3345.
29. Babak, G.; Mohamad, M.; Oromiehie, A.R.; Keramat, R.; Elhame, R.R.; Jafar, M. Effect of plasticizing sugars on water vapor permeability, surface energy and microstructure properties of zein films. *LWT* **2007**, *40*, 1191–1197.
30. Soliman, E.A.; Khalil, A.A.; Deraz, S.F.; El-Fawal, G.; Abd Elrahman, S. Synthesis, characterization and antibacterial activity of biodegradable films prepared from Schiff bases of zein. *J. Food Sci. Technol.* **2014**, *51*, 2425–2434. [[CrossRef](#)]
31. Bezawit, A.A.; Tiruzer, B.; Kefyalew, A.G.; Assefa, B.A. Evaluation of Wound Healing Activity of 80% Hydromethanolic Crude Extract and Solvent Fractions of the Leaves of *Urtica simensis* in Mice. *J. Exp. Pharmacol.* **2022**, *4*, 221–241.

32. Sijun, L.; Hongbin, Z.; Wei, Y. Simultaneously improved strength and toughness in  $\kappa$ -carrageenan/polyacrylamide double network hydrogel via synergistic interaction. *Carbohydr. Polym.* **2020**, *230*, 115596.
33. Hai, C.Y.; Chen, Y.L.; Miao, D.; Yihu, S.; Zi, L.W.; Qiang, Z. Improved toughness and stability of  $\kappa$ -carrageenan/polyacrylamide double-network hydrogels by dual cross-linking of the first network. *Macromolecules* **2019**, *52*, 629–638.
34. Yi, D.; Min, H.; Sun, D.; Yi, H.; Yubao, L.; Taosheng, D.; Xiaohong, W.; Zhang, L.; Weizhong, Y. Dual physically cross-linked  $\kappa$ -carrageenan-based double network hydrogels with superior self-healing performance for biomedical application. *ACS Appl. Mater. Interfaces* **2018**, *10*, 37544–37554.
35. Kishore, K.; Santhanalakshmi, K.N. Thermal polymerization of acrylamide by differential scanning calorimetry. *J. Polym. Sci.* **1981**, *19*, 2367–2375. [[CrossRef](#)]
36. Dessouki, A.M.; Taher, N.H.; El-Boohy, H.A. Radiation-induced graft polymerization of acrylamide onto poly (tetrafluoroethylene/Hexafluoropropylene/vinylidene fluoride) (TFB) films. *Int. J. Radiat. Appl. Instrum.* **1990**, *36*, 371–375.
37. Peng, W.; Tan, K.L.; Kang, E.T. Surface modification of poly (tetrafluoroethylene) films via grafting of poly (ethylene glycol) for reduction in protein adsorption. *J. Biomater. Sci. Polym. Ed.* **2000**, *11*, 169–186.
38. Gholam, R.M.; Moslem, M.; Moslem, S.; Mohammad, S. Magnetic- and pH-responsive  $\kappa$ -carrageenan/chitosan complexes for controlled release of methotrexate anticancer drug. *Int. J. Biol. Macromol.* **2017**, *97*, 209–217.
39. Mahmood, W.; Khan, M.; Yee, T. Effects of reaction temperature on the synthesis and thermal properties of carrageenan ester. *J. Phys. Sci.* **2014**, *25*, 123.
40. Hansen, P.E.; Spanget-Larsen, J. NMR and IR investigations of strong intramolecular hydrogen bonds. *Molecules* **2017**, *22*, 552. [[CrossRef](#)]
41. Blume, A.; Hübner, W.; Messner, G. Fourier transform infrared spectroscopy of  $^{13}\text{C}$ : O labeled phospholipids hydrogen bonding to carbonyl groups. *Biochemistry* **1988**, *27*, 8239–8249. [[CrossRef](#)]
42. Elnashar, M.; Hassan, M. Novel epoxy activated hydrogels for solving lactose intolerance. *Biomed. Res. Int.* **2014**, *2014*, 817985. [[CrossRef](#)]
43. Mohamed, T.M.; Sayed, A.; Mahmoud, G.A. Tuning of the properties of polyvinyl alcohol/polyacrylamide film by phytic acid and gamma radiation crosslinking for food packaging applications. *Polym.-Plast. Technol. Mater.* **2023**, *62*, 866–876. [[CrossRef](#)]
44. Meena, R.; Kamalesh, P.; Gaurav, M.; Arup, K.S. Synthesis of the copolymer hydrogel  $\kappa$ -carrageenan-graft-PAAm: Evaluation of its absorbent and adhesive properties. *J. Appl. Polym. Sci.* **2006**, *102*, 5144–5152. [[CrossRef](#)]
45. Sayed, A.; Gehan, S.; Manar, A.; Ghada, A.M. Alkali-cellulose/Polyvinyl alcohol biofilms fabricated with essential clove oil as a novel scented antimicrobial packaging material. *Carbohydr. Polym. Technol. Appl.* **2023**, *5*, 1000273. [[CrossRef](#)]
46. Yesmin, S.; Arkajyoti, P.; Tarannum, N.; Atiqur, R.; Sarkar, F.A.; Mir, I.I.W.; Talha, B.; Shafayet, A.S. Membrane stabilization as a mechanism of the anti-inflammatory activity of ethanolic root extract of Choi (*Piper chaba*). *Clin. Phytoscience* **2020**, *6*, 59. [[CrossRef](#)]
47. Toubia, K.; Muhammad, S.; Muhammad, U.M.; Syed, A.S.; Nazish, J.; Shahzeb, K.; Zahid, H.; Arshad, M.; Mubeen, K.; Haroon, R. Self-crosslinked chitosan/ $\kappa$ -carrageenan-based biomimetic membranes to combat diabetic burn wound infections. *Int. J. Biol. Macromol.* **2022**, *197*, 157–168.

**Disclaimer/Publisher's Note:** The statements, opinions and data contained in all publications are solely those of the individual author(s) and contributor(s) and not of MDPI and/or the editor(s). MDPI and/or the editor(s) disclaim responsibility for any injury to people or property resulting from any ideas, methods, instructions or products referred to in the content.